

Comprehensive Evaluation of a Novel Volatile Corrosion Inhibitor Formulation for St37 Carbon Steel in Chloride Media

Ertuğrul Kaya^{1,2}, Ahmet Korkmaz¹, Eslem Dinç², Husnu Gerengi²

¹3-S Engineering Consultation Industry and Commerce Incorporated Company, Düzce, Türkiye

²Corrosion Research Laboratory, Department of Mechanical Engineering, Faculty of Engineering, Düzce University, Düzce, Türkiye

Email: ekaya@3-s.com.tr

How to cite this paper: Kaya, E., Korkmaz, A., Dinç, E. and Gerengi, H. (2025) Comprehensive Evaluation of a Novel Volatile Corrosion Inhibitor Formulation for St37 Carbon Steel in Chloride Media. *Journal of Surface Engineered Materials and Advanced Technology*, **14**, 1-20.

<https://doi.org/10.4236/jsemat.2025.151001>

Received: January 1, 2025

Accepted: January 28, 2025

Published: January 31, 2025

Copyright © 2025 by author(s) and Scientific Research Publishing Inc. This work is licensed under the Creative Commons Attribution International License (CC BY 4.0).

<http://creativecommons.org/licenses/by/4.0/>



Open Access

Abstract

In this research, the influence of a volatile corrosion inhibitor (VCI) blend, which includes boron-amine complex, carboxylic acid, and ester groups, on the corrosion behavior of St37 carbon steel in a 3.5% NaCl solution was assessed. To determine how well the VCI protects against corrosion, electrochemical impedance spectroscopy (EIS) and Tafel polarization (TP) tests were performed. Moreover, tests following the TL-8135-0043 standard were carried out to confirm the effectiveness of the inhibitor. In addition, scanning electron microscopy (SEM) and energy-dispersive X-ray spectroscopy (EDAX) were employed to investigate the protective coating created by the inhibitor on the steel's surface. The EIS findings indicated a notable enhancement in corrosion resistance correlating with higher VCI concentrations. Analysis of Nyquist plots revealed that the VCI provided 71.24% protection. Characterization results illustrated that the inhibitor adheres to the surface, which impedes charge transfer and decreases the corrosion rate. TP tests suggested that the VCI functions as an anodic-type inhibitor, mainly inhibiting anodic dissolution. The VCI test was conducted according to the TL-8135-0043 standards, showing no corrosion signs on metal samples covered with VCI-infused paper for up to 30 days. SEM-EDAX and AFM evaluations affirmed the inhibitor's adhesion to the metal surface, leading to the development of a protective layer.

Keywords

Carbon Steel, St37, Volatile Corrosion Inhibitor (VCI)

1. Introduction

Atmospheric corrosion happens because of the interaction between oxygen, hu-

midity, and harmful substances like acid rain, hydrogen sulfide, and chlorides with metal surfaces [1]. A common approach to safeguard metals from atmospheric corrosion involves the use of corrosion inhibitors. These substances effectively lower corrosion rates even at minimal concentrations and are commonly employed in various sectors, such as oil, gas, water systems, metalworking fluids, coatings, and packaging [2]-[4].

This research examines volatile corrosion inhibitors (VCIs), which possess adequate vapor pressure to evaporate and shield metal surfaces by creating a protective layer that restricts the entry of harmful substances. VCIs are frequently utilized in packaging materials, plastic coatings, and processing liquids to avert atmospheric corrosion while in storage and transit. Their success is influenced by elements like volatility, concentration of the inhibitor, environmental conditions, and UV radiation exposure [5]-[8].

VCIs prevent corrosion by adsorbing onto metal surfaces and creating a protective barrier that limits the entry of harmful ions, all while keeping the metal's characteristics unchanged. For a VCI to work well, it needs to be volatile enough to quickly reach the metal surface and provide protection. The rate at which it evaporates is vital in reducing corrosion, making volatility a critical feature that sets it apart from other inhibitors. VCIs provide an effective and simple approach to managing corrosion in closed spaces and should be safe and non-toxic. When applied correctly, they can enhance the lifespan of equipment without causing localized corrosion like pitting [9]-[11].

A significant number of contemporary VCI formulations prioritize environmental sustainability by being non-toxic and biodegradable. However, it is imperative to acknowledge that the environmental impact of VCIs can vary depending on their chemical composition. It is noteworthy that certain conventional VCIs may contain nitrites or other compounds, which, if not managed with the requisite diligence, have the potential to pose environmental hazards. With respect to human safety, the toxicity of VCIs is contingent upon their concentration and the duration of exposure. It is noted that although high doses or pure samples of certain VCI compounds have the potential to be harmful, the concentrations used in commercial applications are generally low and considered safe [9]. Nevertheless, it is recommended that VCIs be handled in accordance with the manufacturer's guidelines, particularly in industrial settings where there is a possibility of prolonged exposure.

The effectiveness of VCIs depends on factors such as ambient temperature, humidity, inhibitor concentration, application method, and the presence of aggressive ions [11]. Proper selection of metal packaging materials is essential to maintain VCI activity and prevent degradation due to UV exposure [8] [12]. Various chemical compounds have been studied as VCIs, with amines, carboxylic acids, and their mixtures being widely used to protect steel and ferrous metals during storage and transportation [8] [13]. These compounds exhibit a synergistic effect by forming a thicker protective layer that limits ion penetration. Amines and car-

boxylic acids interact through Brønsted-Lowry acid-base reactions and hydrogen bonding, stabilizing as ionic complexes, particularly in the presence of excess carboxylic acid [14]-[17].

In commercial applications, amine-carboxylic acid-based VCIs are incorporated into films, coatings, greases, cleaning solutions, hydrotest fluids, concrete, and capsules [16]. Controlled-release systems utilize carriers such as diatomaceous earth and zeolites. The protective effect of amine-based inhibitors arises from their hydrophobic adsorption layer, which shields metal surfaces from corrosive agents. VCI-containing bags and papers are commonly used for wrapping metal components during storage and transport [13] [14] [18] [19].

Vuorinen and Skinner demonstrated that electron density affects inhibitory efficiency and that shorter-chain ammonium carboxylates are more effective [20]. Hassan *et al.* showed that the benzene ring enhances corrosion inhibition, with benzophenone being the most effective due to its large molecular size [21]. Ram-melt *et al.* investigated the passivation of mild steel using carboxylates, amines, and azoles, demonstrating that their inhibition mechanism depends on pH and environmental pollutants [13]. Quraishi and Jamal synthesized organic VCIs and found that the presence of amine and carboxylate functional groups significantly improved inhibition efficiency [22]. Mikhailovski *et al.* conducted field tests on commercial VCIs in various atmospheres, showing that their protection value decreases over time but remains effective in sealed environments [23]. Wan *et al.* proposed a modified evaluation method for VCI effectiveness [24], while Lavanya *et al.* identified octylcaprylamide and dicyclohexylaminebenzotriazole as the best inhibitors for steam and Cl₂ environments [25]. Focke and co-workers analyzed amine-carboxylic acid-based VCIs and found that their vapor composition changes over time [26]. Zhang *et al.* synthesized bis-piperidiniummethyl-urea as a VCI for carbon steel, confirming its protective film formation via EIS studies [27].

In this research, a VCI mixture that incorporates amine-carboxylic acid and carboxylic acid esters was created. The effectiveness of its corrosion protection was evaluated through the GERMAN TL-8135-0043 test. To evaluate how effectively the newly created VCI formulation penetrates, electrochemical impedance spectroscopy (EIS) and Tafel polarization (TP) tests were thoroughly carried out on St37 low-carbon steel samples that were soaked in a glycerin-water mixture. After the electrochemical evaluations, SEM-EDAX and AFM evaluations were performed on the metal surface, leading to the development of a protective layer.

2. Material and Methods

2.1. Working Electrode and Conducting Electrochemical Experiments

The St37 carbon steel used for the electrochemical and VCI test experiments was obtained from Ereğli Demir Çelik and cut cylindrically with a surface area of 0.75 cm². The specimens employed in this investigation were prepared from St37 steel

having a chemical composition of (wt%): Carbon (C) 0.17, Manganese (Mn) 1.40, Phosphorus (P) 0.05, Silisium (Si) 0.30, Sulphur (S) 0.05 and the balance Iron (Fe) [28]. Before conducting experiments, the surface of the working electrodes was readied by progressively polishing them using sandpaper with different grits ranging from 400 to 2000. Following the sanding process, the metal surface was thoroughly rinsed with distilled water and subsequently placed in the experimental setup [29]. The working electrode, counter electrode, and reference electrode were positioned within a corrosion cell containing a 3.5% NaCl solution. The corrosion behavior of St37 low carbon steel in 3.5% NaCl solution was analyzed using electrochemical impedance spectroscopy (EIS) and Tafel polarization (TP) method at 25 °C for a period of 2 h. These measurements were conducted with a GAMRY 1010 E potentiostat/galvanostat/ZRA system. EIS experiments were performed within a frequency range of 100 kHz to 0.1 Hz, and the acquired impedance data were analyzed using ZsimpWin 3.21 software [30]. TP curves were created by scanning in both the negative and positive directions at a rate of 1 mV/s across a potential span of ± 300 mV.

2.2. Content of VCI and Conducting VCI Experiments

The corrosion inhibitors used in VCI tests were provided by DBSE-0511, TRIEST MWB-2110 3-S Engineering Consultation Industry and Commerce Incorporated Company and were employed in both the VCI and electrochemical evaluations. Comprehensive information about the VCI solution is available in TÜRKPATENT (TPE) patent Application No: 2025/002727 titled “Volatile Corrosion Inhibitor Coating Solution” [31]. **Table 1** presents the details of the VCI formulation that was applied in the experiments.

Table 1. Content of VCI formulation.

Sample	% (by weight)
TRiest DBSE-0511	1 - 10
C6 carboxylic acid	1 - 10
TRiest MWB-2110	10 - 40
Isopropyl alcohol (IPA)	30 - 60
Butyl diglycol (BDG)	1 - 10

VCI paper used in VCI tests was supplied from Çağdaş Kraft Paper. These papers were impregnated with corrosion inhibitors by dipping and VCI tests were performed. The VCI test was conducted in accordance with the German standard TL-8135-0043 to assess the effectiveness of VCI products in protecting metal surfaces from corrosion. This test aims to quantify and compare the protective performance of specific VCI formulations on metals, playing a crucial role in the development of anti-corrosion solutions, particularly for automotive and industrial applications. For the test, metal samples typically composed of iron, steel, or alu-

minum were prepared, with St37 carbon steel selected as the test material in this study.

The metal pieces were trimmed to a size of 12 mm in length and 16 mm in diameter, in accordance with the standard specifications. To achieve a smooth finish, the trimmed pieces were sanded and treated with a combination of alcohol and water before being inserted into a rubber stopper. This stopper had a top diameter of 53 mm, a bottom diameter of 45 mm, and a central opening that measured 15 mm across to fit the metal pieces. A VCI paper was attached to a wire that was 15 mm long, and connected to the rubber stopper, which was then placed into a wide-mouth flask following the DIN 12385 standard. A corrosive solution made from a glycerin and water mix (32% and 78% by volume) was poured into the flask. The entire assembly was left at room temperature for 2 hours, then placed in an oven set to 40 °C for another 2 hours. After this heating phase, the rubber stopper was taken out of the flask, and the metal surface was inspected for any corrosion.

3. Results and Discussion

3.1. EIS Measurements

The solubility of the VCI formulation in 3.5% NaCl solution was observed to be high. The corrosion inhibition performance of the VCI formulation at varying concentrations was assessed for St37 carbon steel in a 3.5% NaCl environment at 25 °C over a one-hour exposure period using EIS. The Nyquist plot, obtained from the EIS measurements, illustrates the impact of different concentrations of the VCI formulation in 3.5% NaCl solution (**Figure 1(a)**). At high frequencies, the Nyquist spectra displayed a semicircular-like shape, a typical characteristic of charge transfer-controlled corrosion processes (**Figure 1(a)**) [32]. The analysis of Nyquist plots for both the control system and the samples treated with VCI showed that adding the VCI formulation resulted in a significant rise in the magnitude of the semicircle. This increase, which correlated with inhibitor concentration, demonstrated the corrosion inhibition capability of the VCI formulation [33][34]. The proportional expansion of semicircles with increasing VCI concentration suggests that an optimal inhibition efficiency can be achieved through precise formulation adjustments. It is proposed that segments of the VCI formulation adhere to the metal surface through chelation or hydrogen bonding, facilitated by carboxylic acid and boron-amine complexes. This adsorption mechanism likely contributes to the inhibition effect by obstructing active reaction sites and reducing charge transfer. The deviation from perfect semicircular behavior in the Nyquist plots is attributed to the frequency dispersion of the interfacial impedance, a phenomenon frequently discussed in the literature [35]. Contributing factors include: 1) surface roughness of the working electrode, 2) heterogeneity of the substrate, 3) impurities in the metal or electrolyte, 4) grain boundaries, 5) formation of surface layers, and 6) adsorption of corrosion products or inhibitor molecules [35]-[37].

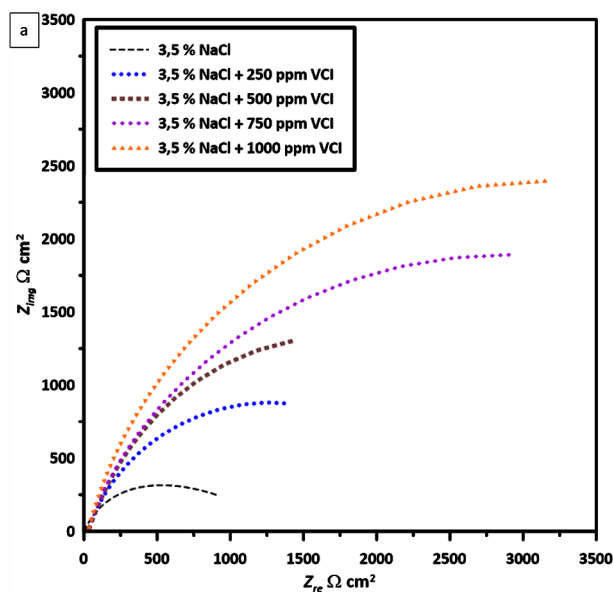
The Bode modulus plot (**Figure 1(b)**) aligns with the trends observed in the Nyquist diagrams. As the inhibitor concentration increases, the impedance shifts towards more noble values, indicating improved corrosion resistance. Additionally, the phase angles (**Figure 1(c)**) consistently approach 70° at all inhibitor concentrations, ruling out significant diffusion effects [33].

To quantify the corrosion resistance of St37 carbon steel in 3.5% NaCl solution and the effectiveness of the VCI formulation, Nyquist spectra were analyzed using an $R(QR)$ equivalent circuit. Data analysis was conducted with ZSimpWin 3.21 software. The chi-square (χ^2) value, which indicates the goodness of fit between experimental and simulated data, was minimized, confirming the accuracy of the impedance model. The electrochemical impedance parameters are summarized in **Table 2**. As the inhibitor concentration increased, parameter n approached unity, suggesting capacitive behavior of the substrate surface [38] [39]. The charge transfer resistance (R_{ct}) values were significantly higher in inhibitor-containing solutions compared to the blank system, with a direct correlation between R_{ct} and inhibitor concentration. Conversely, the double-layer capacitance (C_{dl}) exhibited an inverse relationship with R_{ct} , further confirming that the inhibition effect stems from the adsorption of the VCI formulation and the progressive formation of a protective layer on the metal surface [27]. The inhibition efficiency (IE%) of VCI formulation in the studied environment was computed using Equation (1) [40].

$$IE = \left(1 - \frac{R_{ct}^0}{R_{ct}}\right) \times 100 \quad (1)$$

where R_{ct}^0 is the charge transfer resistance in the absence of VCI formulation and R_{ct} is the charge transfer resistance in the presence of VCI formulation.

Figure 1 shows EIS spectra of (a) Nyquist, (b) Bode modulus and (c) Phase angle representations for St37 carbon steel in 3.5% NaCl solution in the absence and presence of VCI formulation at different concentrations.



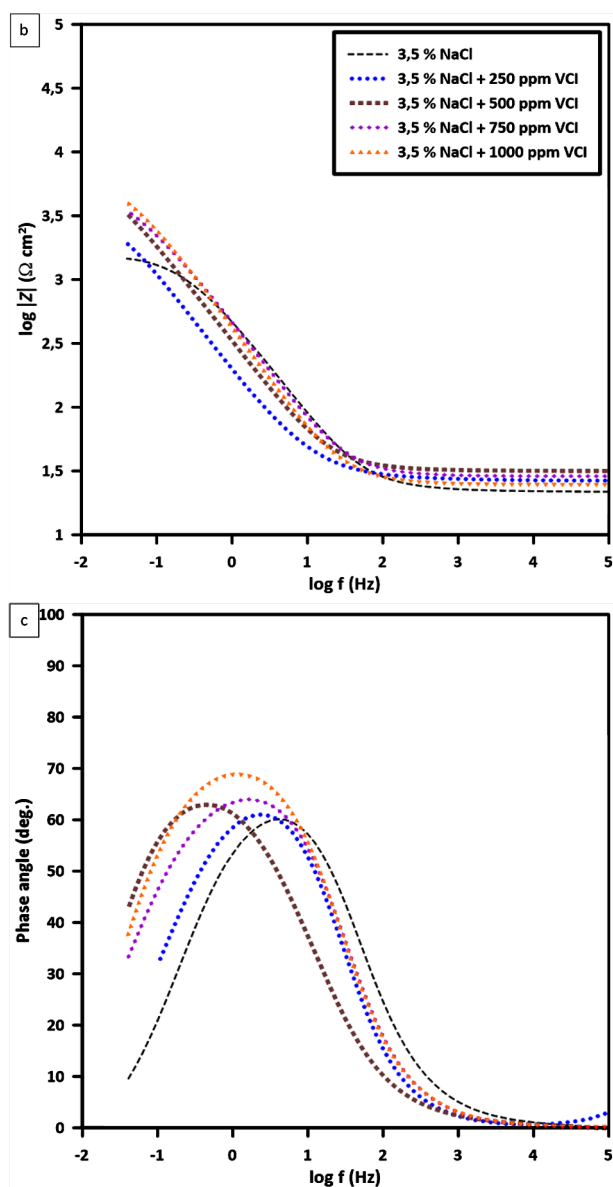


Figure 1. EIS spectra of (a) Nyquist, (b) Bode modulus and (c) Phase angle representations for St37 carbon steel in 3.5% NaCl solution in the absence and presence of VCI formulation at different concentrations.

Table 2. EIS result of different concentrations of VCI formulation in 3.5% NaCl solution of St37 carbon steel.

Inhibitor concentration	CPE				
	R_s ($\Omega \text{ cm}^2$)	Y_0 ($\Omega^{-1} \text{ s}^2 \text{ cm}^{-2}$)	$n_0 \leq n \leq 1$	IE (%)	Chi-square
3.5 % NaCl	1.02	0.0002696	0.75	-	8.980E-4
3.5 % NaCl + 250 ppm VCI	1.12	0.00002016	0.83	33.96	8.665E-4
3.5 % NaCl + 500 ppm VCI	1.15	0.00001983	0.84	36.40	9.108E-4
3.5 % NaCl + 750 ppm VCI	1.09	0.00001251	0.88	68.21	9.052E-4
3.5 % NaCl + 1000 ppm VCI	1.19	0.00001096	0.90	71.24	8.519E-4

Table 2 presents the electrochemical parameters, including R_s , which represents the solution resistance for St37 carbon steel in 3.5% NaCl solution, measured at $1.02 \Omega \cdot \text{cm}^2$. In the presence of the VCI formulation, both R_s and R_{ct} values increased, while the Q parameter of the constant phase element (CPE) decreased. Specifically, in the absence of the inhibitor, R_{ct} was recorded at $953.16 \Omega \cdot \text{cm}^2$ with a Q value of $0.0002696 \Omega^{-1} \text{ s}^2 \text{ cm}^{-2}$. Upon the addition of 250 ppm VCI, R_s and R_{ct} increased to $1.12 \Omega \cdot \text{cm}^2$ and $1443.29 \Omega \cdot \text{cm}^2$, respectively, while Q declined to $0.0002016 \Omega^{-1} \text{ s}^2 \text{ cm}^{-2}$. Similarly, at 1000 ppm VCI concentration, R_s and R_{ct} were even more elevated to $1.19 \Omega \cdot \text{cm}^2$ and $3313.75 \Omega \cdot \text{cm}^2$, respectively, while Q decreased to $0.00001096 \Omega^{-1} \text{ s}^2 \text{ cm}^{-2}$. The inhibition efficiency ($\% \eta_{EIS}$) at the highest studied concentration reached 71.24% in 3.5% NaCl solution.

The corrosion resistance conferred by the VCI formulation is attributed to its molecular structure, which contains a significant number of π -electrons along with nitrogen and boron elements. These features play a vital role in preventing iron corrosion in aggressive environments. The delocalized π -electrons facilitate coordination bond formation with the metal surface, enhancing inhibitor adsorption. Under corrosive conditions, the negatively charged iron surface interacts with nitrogen and boron moieties, enabling the anchoring of ester and carboxylic acid chains. The bulky nature of the ester and boron-amine complex promotes the formation of a cluster-like network on the iron surface, reinforcing adsorption strength and improving surface coverage, thereby enhancing inhibition efficiency [39] [41].

3.2. TP Measurements

As shown in **Figure 2**, the formulation of the VCI affects both the oxidation at the anode and the reduction of hydrogen at the cathode. The change in E_{corr} caused by the inhibitor was more significant than in the system without the inhibitor, rising from -791 mV to -483.7 mV . This change indicates that the groups of carboxylic acid, ester, and boron-amine complex found in the VCI formulation primarily act as an anodic-type inhibitor in the process of preventing corrosion. The presence of the VCI formulation in the corrosive medium effectively mitigated Cl^- -induced attack on St37 carbon steel. In particular, the samples exposed to the VCI formulation demonstrate an increase in current density within the initial passive potential regions (highlighted by red circles) until a maximum is attained, accompanied by an increase in corrosion potential. This phenomenon can be attributed to the initial rapid attack of the metal surface by hydroxyl ions. Such observations may be indicative of inhomogeneous adsorption on the surface, as well as transient adsorption-desorption imbalances [42]-[44].

However, as the inhibitor concentration increased, anodic current densities demonstrated a decreasing trend [45]. The observed E_{corr} values further confirm that the VCI formulation primarily acts as an anodic inhibitor by significantly reducing the anodic dissolution rates of St37 carbon steel while exerting minimal influence on cathodic hydrogen evolution. This strongly supports the assertion that

the inhibitor regulates anodic reactions and functions as an anodic-type corrosion inhibitor [42] [45].

Table 3. TP result of different concentrations of VCI formulation in 3.5% NaCl solution of St37 metal.

Inhibitor concentration	β_a (mV/Dec)	β_c (mV/Dec)	E_{corr} (mV/Ag/AgCl)	I_{corr} ($\mu\text{A}/\text{cm}^2$)	CR (mmpy)	IE (%)
3.5 % NaCl	193.2	385.5	-791.0	121.30	110.4	-
3.5 % NaCl + 250 ppm VCI	170.4	345.3	-788.6	85.49	76.5	29.52
3.5 % NaCl + 500 ppm VCI	203.8	378.3	-596.6	76.07	68.8	37.28
3.5 % NaCl + 750 ppm VCI	181.7	278.2	-561.5	36.60	32.3	69.82
3.5 % NaCl + 1000 ppm VCI	166.3	383.7	-483.7	28.46	25.7	76.53

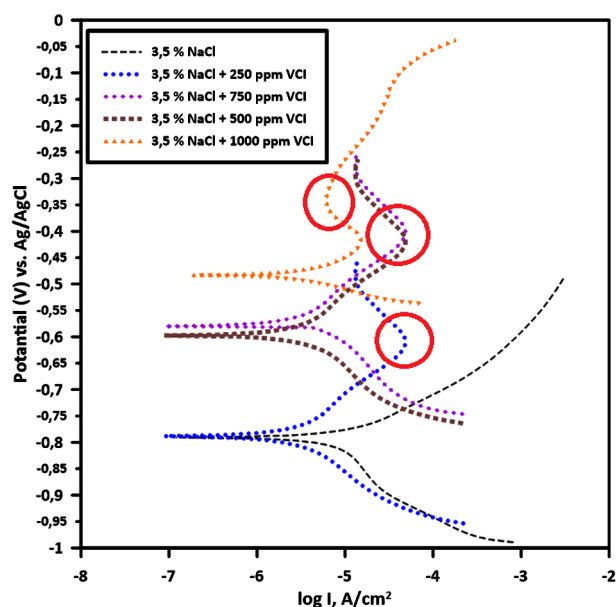


Figure 2. TP plots for St37 carbon steel in 3.5% NaCl solution in the absence and presence of VCI formulation at different concentrations.

The data presented in **Table 3** illustrates that adding the VCI formulation to the 3.5% NaCl solution significantly lowered the corrosion current density of the metal. In particular, including 250 ppm of the inhibitor decreased I_{corr} from $121.3 \mu\text{A}/\text{cm}^2$ to $85.49 \mu\text{A}/\text{cm}^2$, achieving a 29.52% inhibition efficiency. The inhibition efficiency (IE%) of VCI formulation in the studied environment was computed [39] [46] [47]. When the VCI concentration went up to 500 ppm, 750 ppm, and 1000 ppm, the corrosion protection efficiency increased to 37.28%, 69.82%, and 76.53%, respectively. These results strongly correlate with the EIS outcomes and further confirm the effectiveness of the VCI formulation in reducing corrosion of St37 carbon steel in 3.5% NaCl environment.

3.3. VCI Test Measurements

A solution was prepared using the components listed in **Table 1** and subsequently

applied to VCI paper that did not contain any pre-existing inhibitor. Following the application, the treated VCI paper was stretched and left to dry under ambient conditions for 1, 7, and 30 days. To evaluate the corrosion protection performance over time, VCI corrosion tests were performed on the VCI-treated paper and the control sample without VCI after each storage period according to the German standard TL-8135-0043 (Figure 3). The results revealed that no visible signs of corrosion appeared on the metal surface after 1, 7 or 30 days of exposure. Corrosion was clearly observed on the paper without VCI. Figure 4 shows images of the VCI test results.



Figure 3. German standard TL-8135-0043 test.



Figure 4. German standard TL-8135-0043: Corrosion Evaluation of Samples Without VCI and Protected with VCI Formulation (1, 7, and 30 days).

These findings highlight the sustained effectiveness of the VCI formulation in preventing metal degradation over an extended period. Corrosion is a complex electrochemical process driven by environmental factors, particularly in chloride, oxygen, and high temperature-containing atmospheres, which accelerate metal oxidation and deterioration [48]. The absence of corrosion in the tested samples suggests that the VCI paper, impregnated with the inhibitor-containing solution, successfully established a protective barrier that hindered the diffusion of aggressive species such as Cl^- ions [34]. This protective mechanism is likely attributed to the adsorption of active VCI components onto the metal surface, reducing the rate of anodic dissolution and cathodic hydrogen evolution. Furthermore, the stability of the corrosion inhibition effect over 30 days underscores the long-term efficiency of the VCI formulation, making it a promising candidate for industrial

applications requiring prolonged metal protection under harsh conditions.

3.4. SEM-EDAX and AFM Studies

The SEM analysis of St37 carbon steel following electrochemical impedance spectroscopy (EIS) experiments in a 3.5% NaCl solution is presented in **Figure 5**. In **Figure 5(a)**, the surface of the metal appears smooth with visible marks from the sanding process, but no significant corrosion damage is observed. However, when exposed to the corrosive environment, as shown in **Figure 5(b)**, the metal surface shows deterioration. **Figure 5(c)** shows the effect of the corrosion inhibitor, where the previous degradation appears to have closed, indicating adsorption of the inhibitor molecules on the metal surface.

The elemental composition of these surfaces was further examined EDAX with the corresponding results summarized in **Table 4**. The analysis of the uncorroded metal surface revealed the presence of C (0.15%), Si (0.3%), Mn (1.3%), and Fe (98.25%). However, upon exposure to 3.5% NaCl in the absence of an inhibitor, the concentrations of Mn and Fe significantly decreased to 0.3% and 41.2%, respectively. This reduction is attributed to the formation of corrosion products covering the metal surface. Furthermore, O (43.0%) and Cl (10.4%) were detected on the corroded surface, suggesting the presence of a mixed chloride-oxide corrosion layer [49].

Table 4. EDAX analysis results of St37 carbon steel in 3.5% NaCl solution.

	<i>Fe</i>	<i>O</i>	<i>C</i>	<i>Cl</i>	<i>Na</i>	Mn	Si	B	N
Before experiment	98.25	-	0.15	-	-	1.30	0.3	-	-
After immersion in 3.5% NaCl solution	41.2	43.0	2.5	10.4	2.4	0.3	0.2	-	-
1000 ppm VCI formulation	76.4	5.8	10.0	2.3	1.3	0.2	0.1	2.6	1.3

The addition of a 1000 ppm VCI formulation inhibitor significantly influenced the surface composition. The concentrations of Fe and Mn increased to 76.4% and 0.2%, respectively, indicating reduced corrosion and enhanced surface protection. Concurrently, a notable decrease was observed in the O and Cl content, which dropped to 5.8% and 2.3%, respectively. In **Table 4**, the appearance of N and B in the content of 1000 ppm VCI formulation additive added to 3.5% NaCl medium confirms the adsorption of the additives in the VCI formulation on the St37 metal surface. It is seen that carbon-based compounds (such as carboxylic acid, boron-amine complex ester, and alcohol) in the VCI formulation form a film layer on the surface (**Figure 5(c)**). This reduction further supports the hypothesis that the inhibitor effectively adsorbs onto the metal surface, mitigating the extent of corrosion.

The AFM analysis of St37 carbon steel following EIS experiments in a 3.5% NaCl solution is presented in **Figure 6**. As illustrated in **Figure 6**, the 2D AFM images depict the roughness parameters of the St37 samples. According to the AFM results (**Figure 6(a)**), the surface of St37 metal is depicted prior to the experiment. The mean profile deviation from the center line (R_a) was found to be 1.541 - 2.183 nm, and the mean to the peak height (R_z) was 8.363 - 11.943 nm. These values indicate

that the surface roughness of the metal was minimal prior to the experiment. In the 3.5% NaCl medium (see **Figure 6(b)**), the surface roughness of the surfaces increased

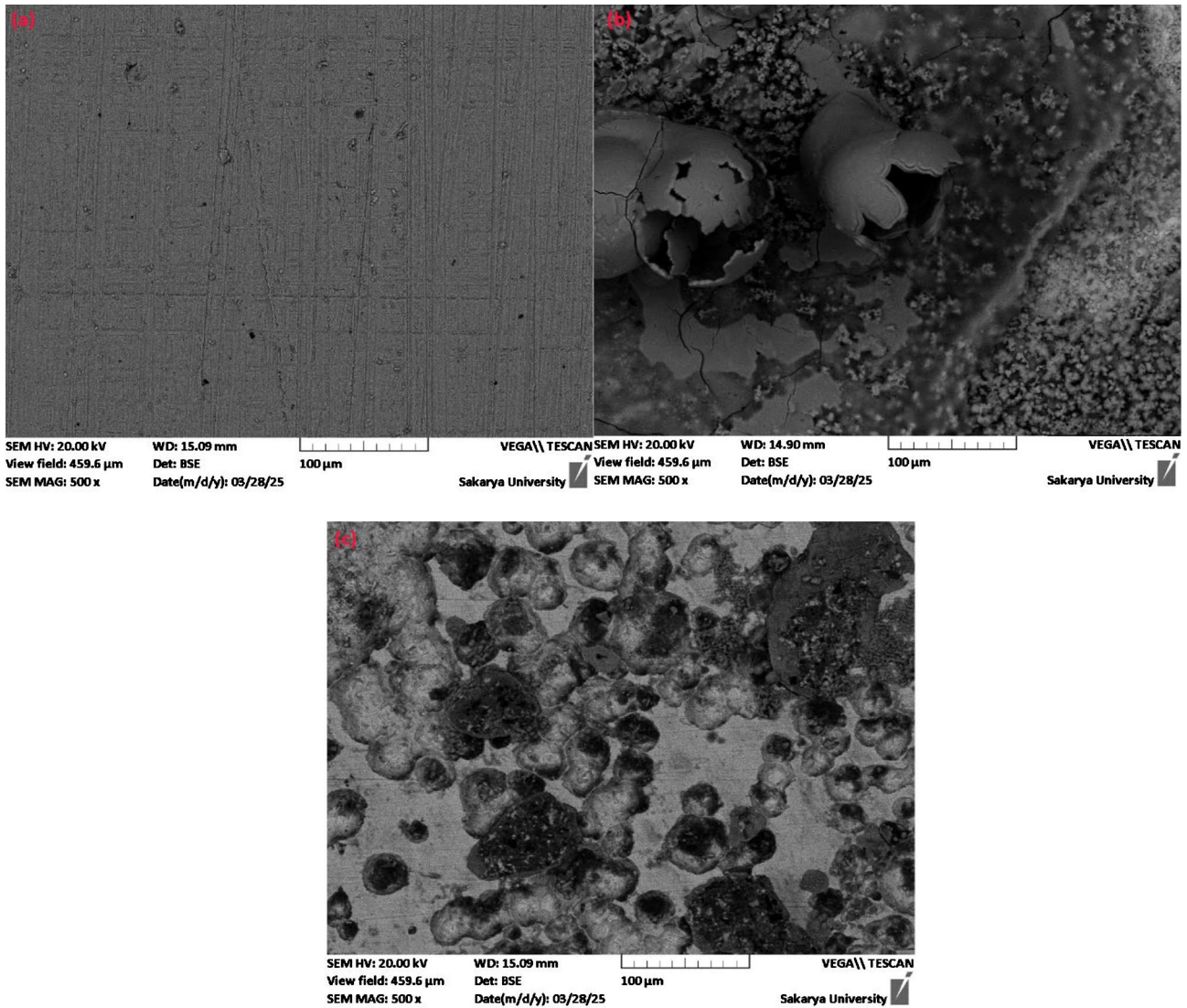
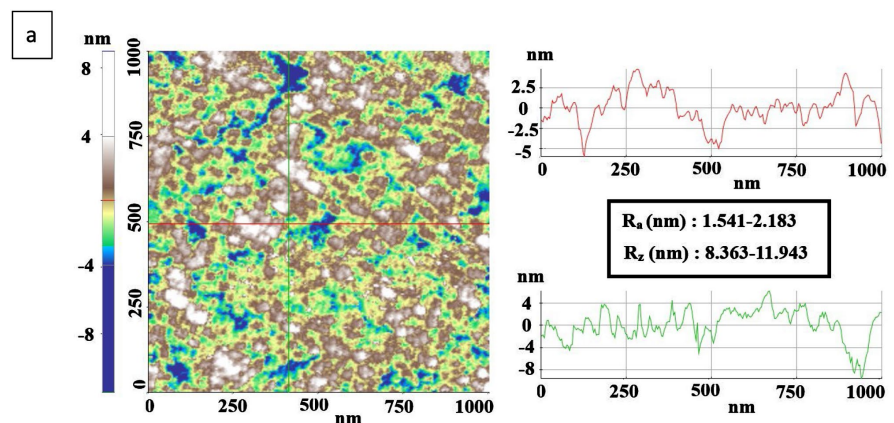


Figure 5. SEM images showing the surface morphology of the St37 carbon steel sample: (a) Before immersion in 3.5% NaCl solution; (b) After immersion in 3.5% NaCl solution; and (c) Containing 1000 ppm VCI formulation.



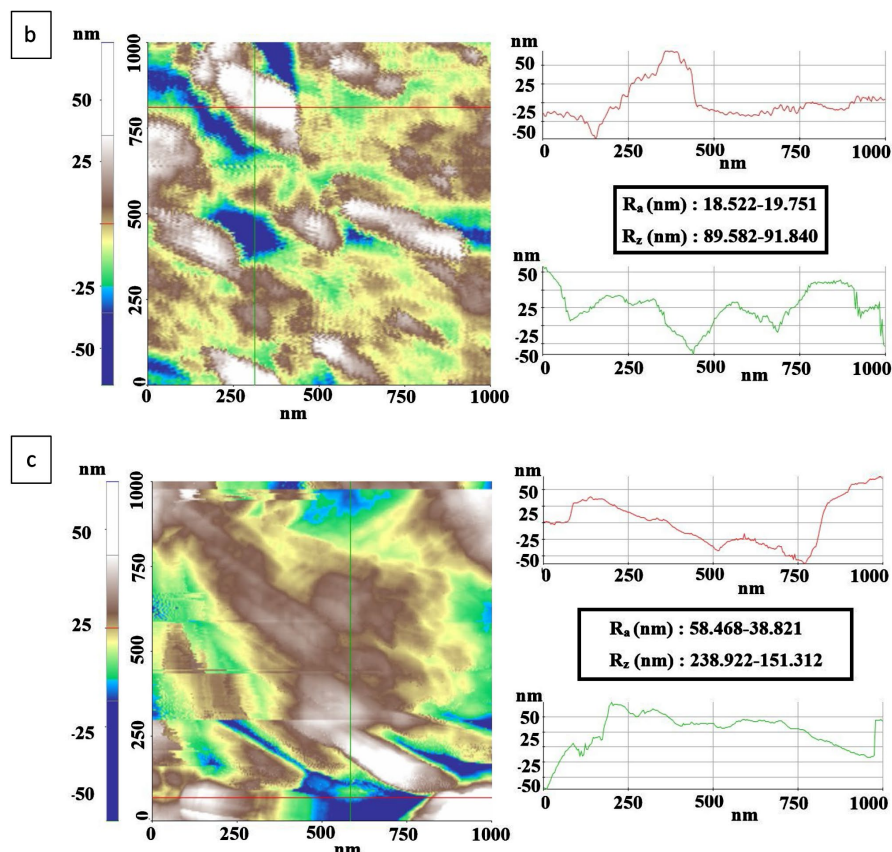


Figure 6. AFM images showing the surface morphology of the St37 carbon steel sample: (a) Before immersion in 3.5% NaCl solution; (b) After immersion in 3.5% NaCl solution; and (c) Containing 1000 ppm VCI formulation.

significantly compared to the surfaces before experiment state. The values of R_a and R_z increased to 38.821 - 58.468 and 151.312 - 238.922 nanometers, respectively. When 1000 ppm VCI formulation was added to the corrosive medium (see **Figure 6(c)**), the R_a and R_z values decreased to 18.522 - 19.751 nm and 89.582 - 91.840 nm, respectively. These results align with the findings from the SEM and electrochemical analysis.

3.5. Protection Mechanisms

The developed VCI formulation is specifically designed to provide protection for both ferrous and non-ferrous metals, including various alloys, industrial machinery, structural components and equipment. VCI molecules effectively diffuse into confined spaces, recesses, crevices, and cavities that are exposed to corrosive environments, such as high humidity and saline atmospheres. The protective mechanism of VCIs is primarily governed by two fundamental chemical processes [50].

Ionization: This process involves the dissociation of VCI molecules, leading to the formation of ions that interact with the metal surface. These ions create a protective barrier by adsorbing onto the metal substrate, mitigating electrochemical reactions responsible for corrosion (Equation (2)) [50].



VCI's undergo hydrolysis, resulting in the cleavage of water molecules into hydrogen cations (H^+) and hydroxide anions (OH^-). This reaction modulates the pH at the metal interface, contributing to passivation and reducing the aggressiveness of corrosive species (Equation (3)) [50].

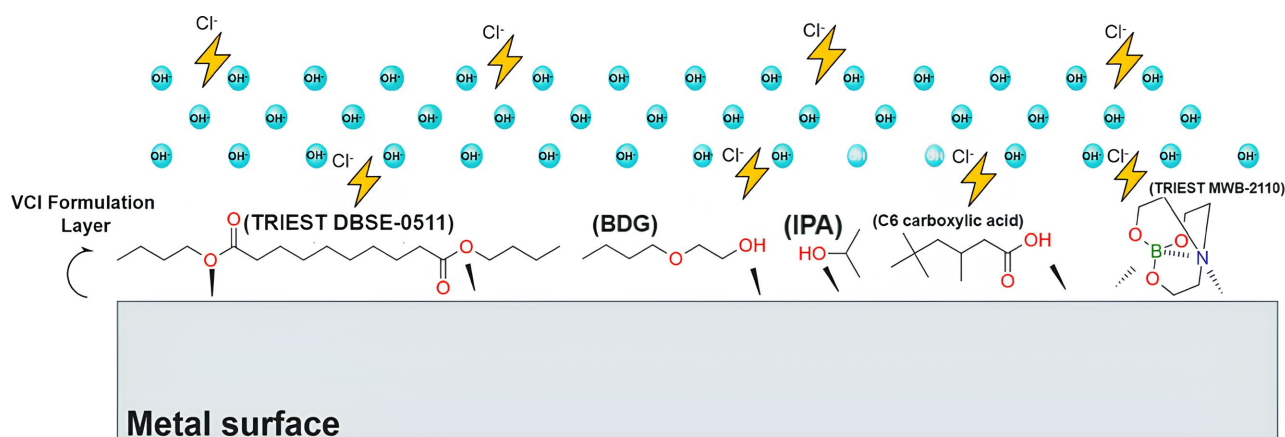
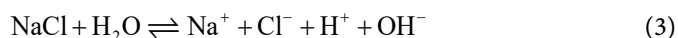


Figure 7. Mechanism of the substances in the VCI formulation as corrosion inhibitors.

Additionally, the efficacy of VCIs is influenced by their molecular structure, volatility, and compatibility with hydrophobic additives such as TRIEST DBSE-0511, which enhances surface adsorption and water displacement properties (Figure 7). Due to its hydrophobic nature, TRIEST DBSE-0511 tends to displace water molecules from the metal surface, reducing water-mediated corrosion [51] [52]. This process leads to the formation of a protective hydrophobic film that limits the diffusion of corrosive species. Additionally, TRIEST DBSE-0511 interacts with the passive oxide layer or adsorbed ions through weak Van der Waals and dispersion forces, promoting surface adherence [53]. The presence of chloride ions (Cl^-) in NaCl solutions can destabilize the passive layer, increasing localized corrosion risks; however, TRIEST DBSE-0511 mitigates this by forming a barrier that limits ion penetration. Furthermore, while TRIEST DBSE-0511 does not strongly coordinate with Fe^{2+} or Fe^{3+} ions, its ester groups can establish weak ion-dipole interactions with Na^+ and Cl^- in solution, enhancing surface adsorption. TRIEST MWB-2110 exhibits strong adsorption characteristics due to the presence of both amine ($-\text{NH}_2$) and borate ($-\text{BO}_3$) functional groups. The amine groups can participate in electrostatic interactions with negatively charged surface oxides and hydroxides, while also forming hydrogen bonds with hydroxyl ($-\text{OH}$) groups on the metal surface [54]. Additionally, the lone pair of electrons on nitrogen allows for coordination bonding with iron atoms, further enhancing adsorption stability [55] [56]. The borate component can also interact with iron oxides, promoting the formation of a protective layer that mitigates corrosion [55]. C6 carboxylic acid is a branched-

chain carboxylic acid that interacts with the metal surface primarily through its carboxyl (-COOH) functional group. The carboxyl group can undergo proton exchange with surface hydroxides, leading to the formation of chemisorbed carboxylate species. This chemisorption enhances the stability of the adsorption layer, contributing to corrosion inhibition [57].

Additionally, C6 carboxylic acid may form hydrogen bonds with hydroxyl (-OH) groups on the oxide layer of the metal surface, further stabilizing its adsorption. The hydrophobic alkyl chain can also contribute to a protective barrier by reducing water penetration and minimizing direct exposure of the metal surface to corrosive agents. In the presence of NaCl, chloride ions (Cl^-) may compete for adsorption sites, potentially disrupting the protective layer formed by C6 carboxylic acid. However, the strong interaction between the carboxylate group and the metal surface helps maintain a stable adsorption, providing some resistance against chloride-induced corrosion [39]. The synergistic interaction between VCI compounds and organic corrosion inhibitors, such as boron amine complexes and carboxylic acid-based molecules, further strengthens their protective performance under dynamic environmental conditions.

4. Conclusions

This study demonstrates the effectiveness of VCI formulations in mitigating the corrosion of low-carbon steel exposed to 3.5% NaCl solution, employing inhibitors such as long-chain esters, boron-amine complexes, short- and medium-chain alcohols, and carboxylic acids. The protective efficiency of these compounds is primarily governed by hydrophobic film formation, Van der Waals interactions, and weak ion-dipole forces rather than strong coordinative bonds. In chloride-containing environments, where passive oxide layers on metals are prone to degradation, the esters and alcohols in the VCI formulation act by creating molecular barriers that hinder water and aggressive ion penetration, thereby mitigating localized corrosion. TRIEST DBSE-0511, for instance, does not establish direct ionic bonds with Fe^{2+} or Fe^{3+} ions but instead displaces surface water, reducing electrolyte access and enhancing corrosion resistance. Similarly, boron-amine complexes and carboxylic acids contribute to passivation by modifying the electrochemical environment and stabilizing protective layers.

Electrochemical results and industrial application data indicate that the developed VCI formulation effectively protects St37 low-carbon steel against corrosion. Overall, the findings underscore the significance of VCI formulations in corrosion prevention, particularly for metals exposed to aggressive environments. By tailoring inhibitor compositions and incorporating synergistic additives, the efficiency of VCI-based protection strategies can be significantly enhanced, making them viable alternatives to conventional corrosion prevention methods in industrial applications. Future research should focus on hybrid VCI formulations that integrate both organic and inorganic components to achieve superior stability, environmental compatibility, and long-term metal protection. To maximize the in-

dustrial potential of this VCI formulation, future studies should focus on evaluating its protective performance across different metal types, optimizing its effectiveness under varying conditions such as temperature, pH, and salinity, and thoroughly assessing its environmental safety. These studies will expand the VCI's use cases and confirm its effectiveness and ecological viability in various industrial settings.

Acknowledgements

This study is a collaborative effort between academia and industry (3-S Engineering Consultation Industry and Commerce Incorporated Company). The authors gratefully acknowledge the financial support provided by TÜBİTAK 2209-B (Project No.: 1139B412402542) and Duzce University Research Fund (Project No.: 2025.04.06.133).

Conflicts of Interest

The authors declare no conflicts of interest regarding the publication of this paper.

References

- [1] Gerengi, H., Maraşlı, M., Coskun, K., Ozdal, V., Uygur, İ. and Aksu, M. (2025) Maintenance of Corroded Silos: A Case Study. *Düzce Üniversitesi Bilim ve Teknoloji Dergisi*, **13**, 234-247. <https://doi.org/10.29130/dubited.1505994>
- [2] Fathima Sabirneeza, A.A., Geethanjali, R. and Subhashini, S. (2014) Polymeric Corrosion Inhibitors for Iron and Its Alloys: A Review. *Chemical Engineering Communications*, **202**, 232-244. <https://doi.org/10.1080/00986445.2014.934448>
- [3] Umoren, S.A. (2009) Polymers as Corrosion Inhibitors for Metals in Different Media—A Review. *The Open Corrosion Journal*, **2**, 175-188. <https://doi.org/10.2174/1876503300902010175>
- [4] Solomon, M.M., Gerengi, H. and Umoren, S.A. (2017) Carboxymethyl Cellulose/Silver Nanoparticles Composite: Synthesis, Characterization and Application as a Benign Corrosion Inhibitor for St37 Steel in 15% H₂SO₄ Medium. *ACS Applied Materials & Interfaces*, **9**, 6376-6389. <https://doi.org/10.1021/acsami.6b14153>
- [5] Pucić, I., Madžar, T. and Jakšić, M. (2006) PIXE Spectroscopy for Determination of Volatile Corrosion Inhibitor Concentration in Anticorrosion Polymer Films. *Monatshefte für Chemie—Chemical Monthly*, **137**, 953-961. <https://doi.org/10.1007/s00706-006-0488-y>
- [6] Choi, H., Song, Y.K., Kim, K.Y. and Park, J.M. (2012) Encapsulation of Triethanolamine as Organic Corrosion Inhibitor into Nanoparticles and Its Active Corrosion Protection for Steel Sheets. *Surface and Coatings Technology*, **206**, 2354-2362. <https://doi.org/10.1016/j.surfcoat.2011.10.030>
- [7] Asmara, Y.P., Suraj, V., Siregar, J.P., Kurniawan, T., Bachtiar, D. and Mohamed, N.M.Z.N. (2017) Development of Green Vapour Corrosion Inhibitor. *IOP Conference Series: Materials Science and Engineering*, **257**, Article ID: 012089. <https://doi.org/10.1088/1757-899x/257/1/012089>
- [8] Cano, E., Bastidas, D.M., Simancas, J. and Bastidas, J.M. (2005) Dicyclohexylamine Nitrite as Volatile Corrosion Inhibitor for Steel in Polluted Environments. *Corrosion*, **61**, 473-479. <https://doi.org/10.5006/1.3280647>

- [9] Gangopadhyay, S. and Mahanwar, P.A. (2018) Recent Developments in the Volatile Corrosion Inhibitor (VCI) Coatings for Metal: A Review. *Journal of Coatings Technology and Research*, **15**, 789-807. <https://doi.org/10.1007/s11998-017-0015-6>
- [10] Vuorinen, E., Kálmán, E. and Focke, W. (2004) Introduction to Vapour Phase Corrosion Inhibitors in Metal Packaging. *Surface Engineering*, **20**, 281-284. <https://doi.org/10.1179/026708404225016481>
- [11] Andreev, N.N. and Kuznetsov, Y.I. (2012) Volatile Inhibitors of Metal Corrosion. I. Vaporization. *International Journal of Corrosion and Scale Inhibition*, **1**, 16-25. <https://doi.org/10.17675/2305-6894-2012-1-1-016-025>
- [12] Bastidas, J.M. and Mora, E.M. (1998) A Laboratory Study of Mild Steel Vapour Phase Corrosion and Its Inhibition by Dicyclohexylamine Nitrite. *Canadian Metallurgical Quarterly*, **37**, 57-65. <https://doi.org/10.1179/000844398109608901>
- [13] Rammelt, U., Koehler, S. and Reinhard, G. (2009) Use of Vapour Phase Corrosion Inhibitors in Packages for Protecting Mild Steel against Corrosion. *Corrosion Science*, **51**, 921-925. <https://doi.org/10.1016/j.corsci.2009.01.015>
- [14] Orzechowski, K., Pajdowska, M., Czarnecki, M. and Kaatze, U. (2007) Complexation and Proton Transfer in the Binary System Propionic Acid-Triethylamine Evidence from the Composition Dependencies of Mixture Properties. *Journal of Molecular Liquids*, **133**, 11-16. <https://doi.org/10.1016/j.molliq.2006.05.007>
- [15] Aravena, R.I. and Hallett, J.P. (2023) Protic Ionic Liquids Based on Fatty Acids: A Mixture of Ionic and Non-Ionic Molecules. *Journal of Molecular Liquids*, **373**, Article ID: 121241. <https://doi.org/10.1016/j.molliq.2023.121241>
- [16] Kohler, F., Atrops, H., Kalali, H., Liebermann, E., Wilhelm, E., Ratkovics, F., et al. (1981) Molecular Interactions in Mixtures of Carboxylic Acids with Amines. I. Melting Curves and Viscosities. *The Journal of Physical Chemistry*, **85**, 2520-2524. <https://doi.org/10.1021/j150617a021>
- [17] Kaya, E. (2025) Synthesis of Plant-Based Ester for Metalworking Fluids and Tribological Performance. *Düzce Üniversitesi Bilim ve Teknoloji Dergisi*, **13**, 430-442. <https://doi.org/10.29130/dubited.1501022>
- [18] Rammelt, U., Koehler, S. and Reinhard, G. (2011) Electrochemical Characterisation of the Ability of Dicarboxylic Acid Salts to the Corrosion Inhibition of Mild Steel in Aqueous Solutions. *Corrosion Science*, **53**, 3515-3520. <https://doi.org/10.1016/j.corsci.2011.06.023>
- [19] Estevão, L.R.M. and Nascimento, R.S.V. (2001) Modifications in the Volatilization Rate of Volatile Corrosion Inhibitors by Means of Host-Guest Systems. *Corrosion Science*, **43**, 1133-1153. [https://doi.org/10.1016/s0010-938x\(00\)00106-2](https://doi.org/10.1016/s0010-938x(00)00106-2)
- [20] Vuorinen, E. and Skinner, W. (2002) Amine Carboxylates as Vapour Phase Corrosion Inhibitors. *British Corrosion Journal*, **37**, 159-160. <https://doi.org/10.1179/000705902225002385>
- [21] Hassan, S.M., Moussa, M.N., El-Tagoury, M.M. and Radi, A.A. (1990) Aromatic Acid Derivatives as Corrosion Inhibitors for Aluminium in Acidic and Alkaline Solutions. *Anti-Corrosion Methods and Materials*, **37**, 8-11. <https://doi.org/10.1108/eb007261>
- [22] Quraishi, M.A. and Jamal, D. (2002) Development and Testing of All Organic Volatile Corrosion Inhibitors. *Corrosion*, **58**, 387-391. <https://doi.org/10.5006/1.3277627>
- [23] Mikhailovskii, Y.N., Popova, V.M. and Marshakov, A.I. (2000) Field and Accelerated Tests of Contact and Volatile Inhibitors of Atmospheric Corrosion with Various Metals. *Protection of Metals*, **36**, 499-504. <https://doi.org/10.1007/bf02764100>
- [24] Wan, H., Huang, H., Zhang, M. and Li, Z. (2005) A Modified Method for Evaluation

- of Materials Containing Volatile Corrosion Inhibitor. *Journal of Central South University of Technology*, **12**, 406–410. <https://doi.org/10.1007/s11771-005-0172-0>
- [25] Lavanya, K., Kannan, P., Palanisamy, K. and Natesan, M. (2014) Comparison Study of Volatile Corrosion Inhibitors in Steam and Cl₂ Gas Environment on Mild Steel. *Arabian Journal for Science and Engineering*, **39**, 5381-5391. <https://doi.org/10.1007/s13369-013-0844-2>
- [26] Focke, W.W., Nhlapo, N.S. and Vuorinen, E. (2013) Thermal Analysis and FTIR Studies of Volatile Corrosion Inhibitor Model Systems. *Corrosion Science*, **77**, 88-96. <https://doi.org/10.1016/j.corsci.2013.07.030>
- [27] Zhang, D., An, Z., Pan, Q., Gao, L. and Zhou, G. (2006) Volatile Corrosion Inhibitor Film Formation on Carbon Steel Surface and Its Inhibition Effect on the Atmospheric Corrosion of Carbon Steel. *Applied Surface Science*, **253**, 1343-1348. <https://doi.org/10.1016/j.apsusc.2006.02.005>
- [28] Solomon, M.M., Gerengi, H., Kaya, T., Kaya, E. and Umoren, S.A. (2016) Synergistic Inhibition of St37 Steel Corrosion in 15% H₂SO₄ Solution by Chitosan and Iodide Ion Additives. *Cellulose*, **24**, 931-950. <https://doi.org/10.1007/s10570-016-1128-2>
- [29] Lahbib, H., Ben Hassen, S., Gerengi, H. and Ben Amor, Y. (2020) Inhibition Effect of *Cynara cardunculus* Leaf Extract on Corrosion of St37 Steel Immersed in Seawater with and without Bleach Solution. *Chemical Engineering Communications*, **208**, 1260-1278. <https://doi.org/10.1080/00986445.2020.1771320>
- [30] Gerengi, H., Cristiani, P., Solomon, M.M., Ilhan-Sungur, E., Yıldız, M. and Slepski, P. (2025) Dynamic Impedance-Based Monitoring of St37 Carbon Steel Corrosion in Sterilized Manganese Broth Medium. *Electrochimica Acta*, **525**, Article ID: 146011. <https://doi.org/10.1016/j.electacta.2025.146011>
- [31] Kaya, E. (2025) Volatile Corrosion Inhibitor Coating Solution. TPE, Application No. 2025/002727. 1-11.
- [32] Li, X., Deng, S., Lin, T., Xie, X. and Du, G. (2017) 2-Mercaptopyrimidine as an Effective Inhibitor for the Corrosion of Cold Rolled Steel in HNO₃ Solution. *Corrosion Science*, **118**, 202-216. <https://doi.org/10.1016/j.corsci.2017.02.011>
- [33] Solomon, M.M., Gerengi, H., Umoren, S.A., Essien, N.B., Essien, U.B. and Kaya, E. (2018) Gum Arabic-Silver Nanoparticles Composite as a Green Anticorrosive Formulation for Steel Corrosion in Strong Acid Media. *Carbohydrate Polymers*, **181**, 43-55. <https://doi.org/10.1016/j.carbpol.2017.10.051>
- [34] Eibl, S. and Reiner, D. (2011) Correlation of Content and Corrosion Protection of Volatile Corrosion Inhibitors in Packaging Material-Regaining Trust in VCI. *Materials and Corrosion*, **62**, 745-752. <https://doi.org/10.1002/maco.200905546>
- [35] Tao, Z., He, W., Wang, S., Zhang, S. and Zhou, G. (2012) A Study of Differential Polarization Curves and Thermodynamic Properties for Mild Steel in Acidic Solution with Nitrophenyltriazole Derivative. *Corrosion Science*, **60**, 205-213. <https://doi.org/10.1016/j.corsci.2012.03.035>
- [36] Al-Amiery, A.A., Mohamad, A.B., Kadhum, A.A.H., Shaker, L.M., Isahak, W.N.R.W. and Takriff, M.S. (2022) Experimental and Theoretical Study on the Corrosion Inhibition of Mild Steel by Nonanedioic Acid Derivative in Hydrochloric Acid Solution. *Scientific Reports*, **12**, Article No. 4705. <https://doi.org/10.1038/s41598-022-08146-8>
- [37] Al-Edan, A.K., Roslam Wan Isahak, W.N., Che Ramli, Z.A., Al-Azzawi, W.K., Kadhum, A.A.H., Jabbar, H.S., et al. (2023) Palmitic Acid-Based Amide as a Corrosion Inhibitor for Mild Steel in 1M HCl. *Heliyon*, **9**, e14657. <https://doi.org/10.1016/j.heliyon.2023.e14657>
- [38] Ling, L., Zhou, Y., Huang, J., Yao, Q., Liu, G., Zhang, P., et al. (2012) Carboxylate-

- terminated Double-Hydrophilic Block Copolymer as an Effective and Environmental Inhibitor in Cooling Water Systems. *Desalination*, **304**, 33-40.
<https://doi.org/10.1016/j.desal.2012.07.014>
- [39] Ince, A., Koramaz, I., Kaya, E. and Karagoz, B. (2023) An Easy Route for Preparation of Carboxylic Acid and Urea Functional Block Copolymer as Corrosion Inhibitor. *Journal of Adhesion Science and Technology*, **38**, 597-617.
<https://doi.org/10.1080/01694243.2023.2240593>
- [40] Gerengi, H., Solomon, M.M., Kurtay, M., Bereket, G., Goksen, K., Yıldız, M., et al. (2017) Electrochemical and Morphological Assessments of Inhibition Level of 8-Hydroxyquinoline for AA2024-T4 Alloy in 3.5% NaCl Solution. *Journal of Adhesion Science and Technology*, **32**, 207-223. <https://doi.org/10.1080/01694243.2017.1350524>
- [41] Ali Fathima Sabirneeza, A. and Subhashini, S. (2012) A Novel Water-Soluble, Conducting Polymer Composite for Mild Steel Acid Corrosion Inhibition. *Journal of Applied Polymer Science*, **127**, 3084-3092. <https://doi.org/10.1002/app.37661>
- [42] Park, J.S., Cho, D.M., Hong, S.G. and Kim, S.J. (2021) Effects of Reducing Atmospheres of Bright Annealing on the Surface and Corrosion Characteristics of Super Duplex Stainless Steel Tubes. *Surface and Coatings Technology*, **423**, Article ID: 127621.
<https://doi.org/10.1016/j.surfcoat.2021.127621>
- [43] Masuda, T., Ikeda, K. and Uosaki, K. (2013) Potential-Dependent Adsorption/Desorption Behavior of Perfluorosulfonated Ionomer on a Gold Electrode Surface Studied by Cyclic Voltammetry, Electrochemical Quartz Microbalance, and Electrochemical Atomic Force Microscopy. *Langmuir*, **29**, 2420-2426. <https://doi.org/10.1021/la304705k>
- [44] Gerengi, H., Cakmak, R., Dag, B., Solomon, M.M., Tuysuz, H.A.A. and Kaya, E. (2020) Synthesis and Anticorrosion Studies of 4-[(2-Nitroacetophenonylidene)-Amino]-Antipyrine on SAE 1012 Carbon Steel in 15 Wt.% HCl Solution. *Journal of Adhesion Science and Technology*, **34**, 2448-2466.
<https://doi.org/10.1080/01694243.2020.1766400>
- [45] Saadawy, M. (2016) Effect of Inorganic Anions on the Pitting Behaviour of Austenitic Stainless Steel 304 in H₂SO₄ Solution Containing Chloride Ion. *International Journal of Electrochemical Science*, **11**, 2345-2359.
[https://doi.org/10.1016/s1452-3981\(23\)16108-6](https://doi.org/10.1016/s1452-3981(23)16108-6)
- [46] Gerengi, H., Sen, N., Uygur, I. and Kaya, E. (2019) Corrosion Behavior of Dual Phase 600 and 800 Steels in 3.5 Wt.% NaCl Environment. *Journal of Adhesion Science and Technology*, **34**, 903-915. <https://doi.org/10.1080/01694243.2019.1688925>
- [47] Gerengi, H., Solomon, M.M., Kaya, E., Bagci, F.E. and Abai, E.J. (2018) An Evaluation of the Anticorrosion Effect of Ethylene Glycol for AA7075-T6 Alloy in 3.5% NaCl Solution. *Measurement*, **116**, 264-272.
<https://doi.org/10.1016/j.measurement.2017.11.030>
- [48] Numin, M.S., Hassan, A., Jumbri, K., Eng, K.K., Borhan, N., Nik M. Daud, N.M.R., et al. (2022) A Recent Review on Theoretical Studies of Gemini Surfactant Corrosion Inhibitors. *Journal of Molecular Liquids*, **368**, Article ID: 120649.
<https://doi.org/10.1016/j.molliq.2022.120649>
- [49] Qiu, Y., Yang, Y., Yang, N., Tong, L., Yin, S., Yu, L., et al. (2022) Corrosion of Iron Covered with Iron Oxide Film by Chlorine and Hydrogen Chloride Gases: A Molecular Dynamics Simulation Study Using the ReaxFF. *Energies*, **15**, Article 4237.
<https://doi.org/10.3390/en15124237>
- [50] Cheng, N., Salas, B.V., Wiener, M.S. and Martinez, J.R.S. (2018) Vapor Inhibitors for Corrosion Protection in Humid and Saline, Natural, and Industrial Environments. In: *Corrosion Inhibitors, Principles and Recent Applications*, InTech, 165-180.

- <https://doi.org/10.5772/intechopen.72815>
- [51] Lin, B., Luo, Z., Liu, C., Liu, X. and Xu, Y. (2017) Effect of Dioctyl Sebacate on Corrosion Behavior of Fine-Grain High-Strength Reinforcement in Simulated Concrete Pore Solutions. *International Journal of Electrochemical Science*, **12**, 8892-8907. <https://doi.org/10.20964/2017.10.52>
- [52] Chapman, J. and Regan, F. (2011) Sebacic and Succinic Acid Derived Plasticised PVC for the Inhibition of Biofouling in Its Initial Stages. *Journal of Applied Biomaterials & Biomechanics*, **9**, 176-184. <https://doi.org/10.5301/jabb.2011.8787>
- [53] Ukaga, I., Okafor, P., Onyechu, I.B., Ikeuba, A.I. and Njoku, D.I. (2023) The Inhibitive Performance of 2,3-Pyrazine Dicarboxylic Acid and Synergistic Impact of KI during Acid Corrosion of 70/30 and 90/10 Copper-Nickel Alloys. *Materials Chemistry and Physics*, **296**, Article ID: 127313. <https://doi.org/10.1016/j.matchemphys.2023.127313>
- [54] Li, R., Li, J., Wang, Y., Chen, J., Lai, Y. and Hu, J. (2024) A Surface Molecular Assembly-Based Composite Inhibitor for Mitigating Corrosion in Dynamic Supercritical CO₂ Aqueous Environment. *Chemical Engineering Journal*, **495**, Article ID: 153193. <https://doi.org/10.1016/j.cej.2024.153193>
- [55] Zhao, Y., Pan, T., Yu, X. and Chen, D. (2019) Corrosion Inhibition Efficiency of Triethanolammonium Dodecylbenzene Sulfonate on Q235 Carbon Steel in Simulated Concrete Pore Solution. *Corrosion Science*, **158**, Article ID: 108097. <https://doi.org/10.1016/j.corsci.2019.108097>
- [56] Mohamed, A., Martin, U., Visco Jr., D.P., Townsend, T. and Bastidas, D.M. (2023) Interphase Corrosion Inhibition Mechanism of Sodium Borate on Carbon Steel Rebars in Simulated Concrete Pore Solution. *Construction and Building Materials*, **408**, Article ID: 133763. <https://doi.org/10.1016/j.conbuildmat.2023.133763>
- [57] Li, Y., Xu, W., Lai, J. and Qiang, S. (2022) Inhibition Effect and Mechanism Explanation of Perilla Seed Extract as a Green Corrosion Inhibitor on Q235 Carbon Steel. *Materials*, **15**, Article 5394. <https://doi.org/10.3390/ma15155394>